Droplet hurdles race

Hélène de Maleprade, Rafid Bendimerad, Christophe Clanet, David Quéré

Applied Physics Letters ARTICLE scitation.org/journal/apl

Droplet hurdles race

Cite as: Appl. Phys. Lett. **118**, 171601 (2021); doi: 10.1063/5.0043908
Submitted: 12 January 2021 · Accepted: 27 March 2021 ·
Published Online: 27 April 2021

View Online Export Citation CrossMark

Hélène de Maleprade,[1,2] Rafid Bendimerad,[2] Christophe Clanet,[1,2] and David Quéré[1,2,a)]

AFFILIATIONS

[1]Physique and Mécanique des Milieux Hétérogènes, UMR 7636 du CNRS, ESPCI, 75005 Paris, France
[2]LadHyX, UMR 7646 du CNRS, École polytechnique, 91128 Palaiseau, France

[a)]Author to whom correspondence should be addressed: david.quere@espci.fr

ABSTRACT

Water is extremely mobile on non-wetting surfaces, on which it glides at high velocities. We discuss how a few indentations placed on the surface markedly slow down drops forced to hit and jump above these hurdles. The corresponding "friction" is characterized and shown to be inertial in nature, which we interpret as the result of the successive soft shocks of the drops against obstacles.

In 1864, Oxford was facing Cambridge for the first friendly track and field competition during which the standards of the hurdles race were defined.[1] The track was 120 yards-long (∼110 m), with 10 obstacles of 3.5 foot (∼1 m) spaced by 10 yards (∼9 m). The distance was rounded up in 1880, instituting the 110 m hurdles we still know. Merritt holds the current world record, 12.80 s, and an average speed of ∼31 km/h, slower by 20% than the ∼38 km/h of Bolt on a flat track with similar length.[2] In this paper, runners are drops, the athletic track is a water-repellent surface, and hurdles are millimetric indentations that force the liquid to modify its trajectory, as shown in the chronophotography in Fig. 1 and in the supplementary material movie 1.

Water on superhydrophobic materials can reach a velocity on the order of 1 m/s on substrates tilted by a few degrees only,[3,4] a remarkably high speed that qualifies drops as suitable athletes. The very low friction of water on such surfaces offers this extreme mobility,[5–8] which makes drops hard to control.[9–13] However, macroscopic decorations were found to provide solutions to master the liquid dynamics. Hydrophilic lines drawn in a non-wetting landscape are capable of guiding a drop[14] and even stopping it.[15,16] Non-wetting obstacles can also be used for their abilities to dynamically reshape the liquid, as seen with slender textures that redistribute water at impact and shorten the contact time of bouncing drops.[17]

For a drop running into an indentation perpendicular to the motion, the liquid is also reshaped in a discoidal form as it steps over the texture and the velocity decreases after this interaction.[18] On a series of such obstacles, the drop quickly reaches a stationary speed, which can be smaller by a factor of ∼5 compared to that on a smooth surface.[19,20] Obstacles studied so far were either single[18] or dense,[19,20] a case where liquid runners cannot land on the track before facing a new hurdle. Here, we investigate how the drop dynamics is impacted by diluting the obstacles, so that liquid only undergo a few shocks during the race. We will see that this configuration surprisingly slows down water more efficiently than a dense texture. We first describe the dynamics of water droplets before discussing the behavior of more viscous liquids.

As illustrated in Fig. 2(a), drops in our experiments run down a 40-centimeter long superhydrophobic track tilted by an angle α and decorated by indentations with height $H = 1$ mm, thickness 1.5 mm, and spacing $\lambda = 6$, 8, 10, or 12 mm. The distance between obstacles is 4–8 times the texture width, which defines the regime of dilute defects. Tracks are made of aluminum and rendered water-repellent by dipping them into a solution of silanized silica nanobeads with diameter 30 nm (Glaco, Soft99).[21] After solvent evaporation, the coating is consolidated at 250 °C for 30 min. The process is repeated three times to ensure homogeneous surface covering, especially at corners, and the resulting coating exhibits a typical roughness $\Delta z = 100$ nm[21]—a scale smaller by a factor of 10^4 than the indentation (and drop) scale. This treatment provides water repellency, as shown by advancing and receding contact angles, $\theta_a = 171 \pm 2°$ and $\theta_r = 165 \pm 2°$, respectively.

At scales larger than the capillary length $a = \sqrt{\gamma/\rho g}$ (2.7 mm for water), drops are puddles flattened by gravity and have a thickness $\sim 2a$ on non-wetting substrates. As shown in Fig. 2(a), we adjust the drops to the spacing λ, so that their volumes $\Omega \approx \pi a \lambda^2/2$ are around 100 μl. Puddles are made of water–glycerol mixtures (density ρ, surface tension γ, and viscosity η) allowing us to tune at roughly constant ρ and γ the viscosity from 1 to 100 mPa s, corresponding to a glycerol content varying from 0 to 80%. The liquid is gently deposited between two indentations on the tilted track, after which we follow its behavior from the top with a high-speed video-camera Optronis CR600x2, used at typically 200 frames per second.

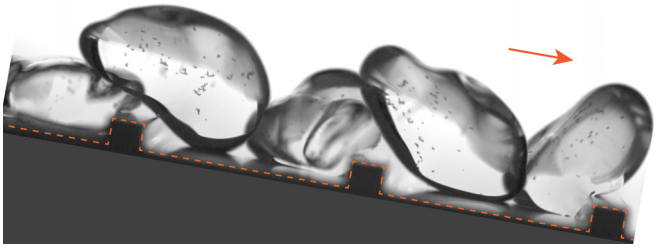

FIG. 1. Chronophotography of "drop hurdles" on a water-repellent track tilted by 12°. The drop volume and viscosity are $\Omega = 100\ \mu l$ and $\eta = 10$ mPa s. The hurdles are indentations with height 1 mm, thickness 1.5 mm, and spacing 8 mm and the track surface is highlighted by dashes. The time between successive images is 30 ms.

As a first obvious observation, the tilt α must be large enough to make the drop run down. The texture generates a gravitational trap that water only overcomes if the hydrostatic pressure generated by the tilt exceeds the Laplace pressure arising from the drop deformation on the texture. For a drop with diameter and height scaling as λ and a, this condition can be written $\rho g \lambda \alpha > \gamma H/a^2$ at small α, which yields a critical angle of motion $\alpha_c \sim H/\lambda$. As seen in Fig. 2(b), the measured angles α_c are indeed proportional to the geometrical factor H/λ. The coefficient of proportionality (obtained after expressing α_c in radians) is found to be 2.10 ± 0.15, a value that might be understood by numerically studying how drops precisely deform against non-wetting indentations.

Above α_c, a drop running down the track accelerates until its velocity saturates, when gravity balances friction. As seen in Fig. 2(c), in supplementary material movie 2 (with $\Omega = 100\ \mu l$ and various α) and in supplementary material movie 3 (with $\alpha = 10°$ and various Ω), this stationary value V increases with both the tilt angle α and with the volume Ω, that is, with the driving weight of the drop. The measured velocities are all comparable or larger than $\sqrt{2gH} \approx 14$ cm/s (indicated with dashes), the value above which inertia enables a drop to pass the hurdles:[18] once set in motion, a drop will run down the whole track.

All dimensions D of the system (λ, a, H) being millimeter-size, the Reynolds number $Re = \rho VD/\eta$ is typically between 10 and 1000, which suggests an inertial origin for the friction. This friction is much larger than on a flat substrate, and we consider that the resistance to the flow arises from the shocks of drops against the substrate, as the liquid falls from an indentation, and when it hits the next indentation. Even on non-wetting materials, such shocks are known to be highly inelastic, as evidenced, for instance, by the poor elasticity of bouncing drops:[22] the energy is transferred in deformations and vibrations and eventually dissipated by viscosity. This dissipative mechanism implies that inertia dominates surface tension, whose effect rigidifies the drop shape. Denoting R as the drop radius, the Weber number $We = \rho RV^2/\gamma$ varies between $\sim$1 and $\sim$10 in our experiments, so that we always expect strong deformations at impact, as indeed seen in the movies.

Despite the complexity of the shapes adopted by the liquid hurdlers (supplementary material movie 1), we simply assume that the kinetic energy lost in the soft shocks is that of the base of the drop, on a height H, that is, $\sim \rho\Omega HV^2/\lambda$. However, the drop in the meantime climbs the obstacle, with an increase $\rho\Omega gH$ in gravitational energy. The total energy penalty can be written as the work of these forces over the distance λ. Balancing it with gravity, $\rho\Omega g\alpha\lambda \approx \rho\Omega HV^2/\lambda + \rho\Omega gH$, provides a stationary drop velocity V at tilt angles larger than α_c:

$$V \approx \sqrt{\frac{g\lambda^2}{H}\,(\alpha - \alpha_c)}. \tag{1}$$

Lines in Fig. 2(c) show Eq. (1) drawn for each volume and adjusted by a common numerical factor of 0.85. The comparison between data and model captures both the variations of the speed in volume and tilt angle. In addition, it must be emphasized that velocities here are much lower (by a factor of 10) than on a non-wetting track without obstacles,[3,4] but also smaller (by a factor of up to 4) than on non-wetting tracks with dense indentations.[19] In the latter case, drops rest on the tops of the obstacles, which minimizes the "shock friction" compared to the present case where the whole drop meets

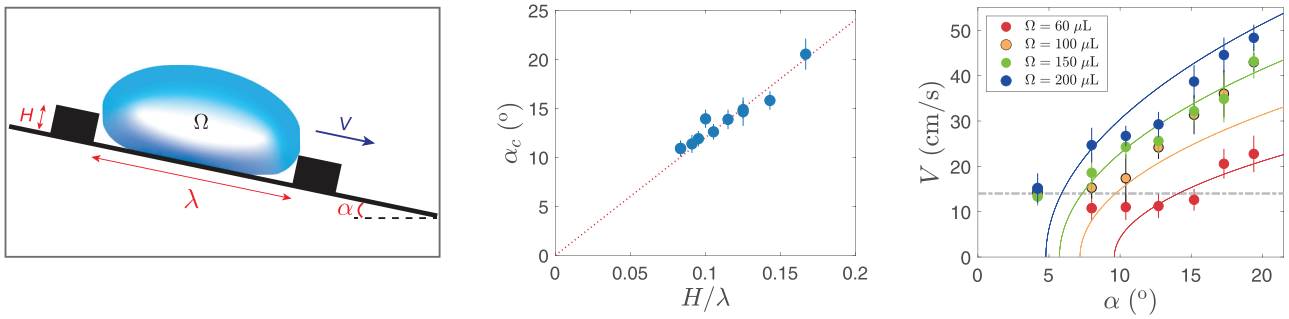

(a) (b) (c)

FIG. 2. (a) Schematic of the experiment: a drop with volume Ω is placed between indentations with height $H = 1$ mm on a tilted non-wetting substrate. At a low tilt angle ($\alpha < \alpha_c$), the drop does not move. Above a critical tilt α_c, the drop quickly acquires a terminal velocity V of a few tens of cm/s. (b) Critical tilt angle α_c (expressed in degrees) as a function of the geometrical ratio H/λ. The drop diameter λ is varied by tuning the drop volume Ω from 80 μl to 200 μl. Error bars correspond to fluctuations in the measurements. (c) Terminal velocity V as a function of the tilt $\alpha > \alpha_c$. Colors specify the indentation period and drop volume: $\Omega = 60\ \mu l$ (red), $\Omega = 100\ \mu l$ (orange), $\Omega = 150\ \mu l$ (green), and $\Omega = 200\ \mu l$ (blue). The lines show Eq. (1) with a numerical factor of 0.85, and the horizontal dashes the velocity $\sqrt{2gH} \approx 14$ cm/s. Error bars indicate the fluctuations in the measurements.

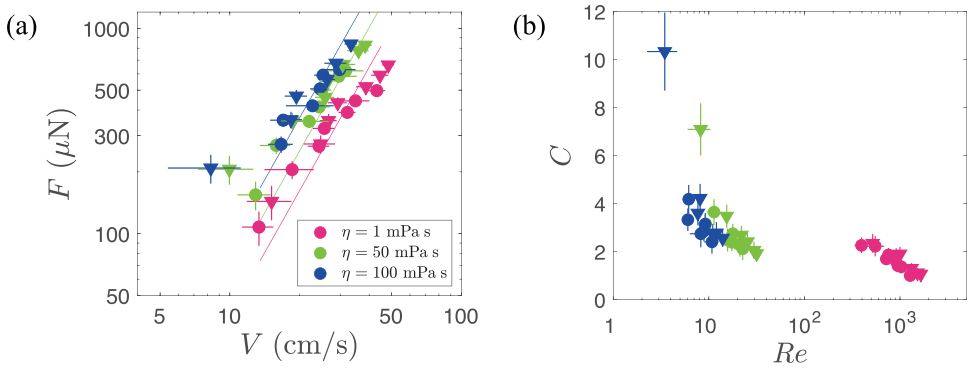

FIG. 3. (a) Friction force as a function of the drop terminal velocity V. Water ($\eta = 1$ mPa s, pink data) and water–glycerol mixtures with viscosity $\eta = 50$ mP s (green data) and $\eta = 100$ mPa s (blue data) are running down non-wetting tracks; the liquid volume is either $\Omega = 150$ μl (triangles) or $\Omega = 200$ μl (disk). Thin lines show the inertial friction force (2) with respective numerical coefficients of 1.6 (for $\eta = 1$ mPa s), 2.1 (for $\eta = 50$ mPa s), and 3.0 (for $\eta = 100$ mPa s). (b) Friction coefficient C, defined as the ratio between the measured friction and the inertial friction (2), as a function of the Reynolds number Re. The color code is the same as in (a).

indentations and eventually explains the high efficiency of hurdles to control the drop speed.

We can finally focus on the original form of the inertial friction force F. For $\alpha > \alpha_c$, it can simply be written $\rho\Omega HV^2/\lambda^2$, which yields

$$F \approx \rho a H V^2. \tag{2}$$

In a stationary regime, this friction is known since it just balances the (known) projection $\rho\Omega g\alpha$ of weight along the track. We plot in Fig. 3(a) its value as a function of the drop velocity, a way to test the inertial behavior assumed in the model. To make the test more complete, we also use various water–glycerol mixtures, so as to increase the liquid viscosity by two orders of magnitude.

Data are obtained in a limited range of velocities (V must be larger than $\sim\sqrt{2gH}$ to get a steady motion, and drops can fragment above ~50 cm/s). However, they suggest a friction independent of the drop volume and quadratic in velocity, as shown by lines with slope 2. In addition, friction varies very little with the viscosity since the numerical coefficient in the fits are, respectively, 1.6 ± 0.4, 2.1 ± 0.3, and 3.0 ± 0.5 as the viscosity passes from 1 to 50 and to 100 mPa s (see supplementary material movie 4 shot at fixed $\Omega = 100$ μl and $\alpha = 12°$, but for different viscosities). This confirms the inertial nature of the friction, even if the drift in the coefficient indicates that viscous effects become non-negligible when the viscosity is around 100 mPa s.

We classically define a friction coefficient C as the ratio between the measured friction and the inertial resistance [expressed in Eq. (2)], $C = F/\rho a H V^2$, which we plot as a function of $Re = \rho RV/\eta$ in Fig. 3(b). Here, Re varies between 6 and 30 for the viscous liquids and between 400 and 1600 for water, and we see again the slight influence of the viscosity in the mean value of C, as we get $C = 1.6 \pm 0.5$ for water, 2.6 ± 0.5 for $\eta = 50$ mPa s, and 3.1 ± 0.6 for $\eta = 100$ mPa s (excluding the two deviating points, at low velocity, where we enter the viscous regime), consistently with the fits in Fig. 3(a). The variations in the friction coefficient are small considering the range of explored Reynolds numbers, but we notice a systematic decrease within each data set. This effect might be a consequence of the small range of velocities we could access, and its quantitative understanding remains to be done.

Finally, a few data at both high η and low V deviate from the fits in Fig. 3(a) and correspond to high C in (b). This can be attributed to the growing influence of viscosity. Mixtures with an even larger viscosity or pure glycerol will run down at a much slower pace and follow a traditional viscous friction, linear in V and η,[23–26] a case where we expect no special effects of the obstacles, in contrast with here. Similarly, if we imagine hurdles with liquid-impregnated surfaces, the viscous dissipation generated on such kinds of materials[27] is expected to screen the additional friction arising from the indentations.

In summary, drops on repellent tracks see their mobility decrease by a factor of order 10 when hurdles are placed on the track. We attribute this effect to a maximization of the inertial friction generated by the soft shocks of the liquid against indentations, which provides a solution for mastering the velocity of non-wetting drops. Even liquids up to 100 times more viscous than water undergo this inertial dissipation, a rather unusual phenomenon made possible by the strong effect of dilute indentations. This effect is somehow reminiscent of that shown for solids falling along a series of cavities, where the energy dissipation similarly takes place in the successive shocks with the obstacles.[28] It would be worth establishing a comparison between both kinds of systems.

See the supplementary material (four movies) for discovering the dynamics of drops with various volumes and viscosities, passing hurdles on tracks with several tilt angles.

DATA AVAILABILITY

The data that support the findings of this study are available from the corresponding author upon reasonable request.

REFERENCES

[1]M. Shearman, "Athletic sports at Oxford and Cambridge Universities," Engl. Illus. Mag. **102**, 441 (1892).
[2]World records, see www.iaaf.org, for "110 Meters Hurdles and 110 Meters, IAAF (2020)"
[3]P. H. Olin, S. B. Lindström, T. Pettersson, and L. Wågberg, "Water drop friction on superhydrophobic surfaces," Langmuir **29**, 9079–9089 (2013).
[4]T. Mouterde, P. Raux, C. Clanet, and D. Quéré, "Superhydrophobic frictions," Proc. Natl. Acad. Sci. U. S. A. **116**, 8220–8223 (2019).

[5]M. Backholm, D. Molpeceres, M. Vuckovac, H. Nurmi, M. J. Hokkanen, V. Jokinen, J. V. I. Timonen, and R. H. A. Ras, "Water droplet friction and rolling dynamics on superhydrophobic surfaces," Commun. Mater. **1**, 64 (2020).
[6]G. Martouzet, C. Lee, C. Pirat, C. Ybert, and A. L. Biance, "Drag reduction on drop during impact on multiscale superhydrophobic surfaces," J. Fluid Mech. **892**, R2 (2020).
[7]J. P. Rothstein, "Slip on superhydrophobic surfaces," Annu. Rev. Fluid Mech. **42**, 89–109 (2010).
[8]R. Blossey, "Self-cleaning surfaces—virtual realities," Nat. Mater. **2**, 301–306 (2003).
[9]P. Hao, C. Lv, Z. Yao, and F. He, "Sliding behavior of water droplet on superhydrophobic surface," Eur. Phys. Lett. **90**, 66003 (2010).
[10]M. Miwa, A. Nakajima, A. Fujishima, K. Hashimoto, and T. Watanabe, "Effects of the surface roughness on sliding angles of water droplets on superhydrophobic surfaces," Langmuir **16**, 5754–5760 (2000).
[11]C.-H. Choi and C.-J. Kim, "Large slip of aqueous liquid flow over a nanoengineered superhydrophobic surface," Phys. Rev. Lett. **96**, 066001 (2006).
[12]P. Joseph, C. Cottin-Bizonne, J.-M. Benoit, C. Ybert, C. Journet, P. Tabeling, and L. Bocquet, "Slippage of water past superhydrophobic carbon nanotube forests in microchannels," Phys. Rev. Lett. **97**, 156104 (2006).
[13]C. Ybert, C. Barentin, C. Cottin-Bizonne, P. Joseph, and L. Bocquet, "Achieving large slip with superhydrophobic surfaces: Scaling laws for generic geometries," Phys. Fluids **19**, 123601 (2007).
[14]H. Hu, S. Yu, and D. Song, "No-loss transportation of water droplets by patterning a desired hydrophobic path on a superhydrophobic surface," Langmuir **32**, 7339–7345 (2016).
[15]P. Olin, S. B. Lindström, and L. Wågberg, "Trapping of water drops by line-shaped defects on superhydrophobic surfaces," Langmuir **31**, 6367–6374 (2015).
[16]D. 't Mannetje, S. Ghosh, R. Lagraauw, S. Otten, A. Pit, C. Berendsen, J. Zeegers, D. van den Ende, and F. Mugele, "Trapping of drops by wetting defects," Nat. Commun. **5**, 3559 (2014).
[17]J. C. Bird, R. Dhiman, H.-M. Kwon, and K. K. Varanasi, "Reducing the contact time of a bouncing drop," Nature **503**, 385–388 (2013).
[18]X. Jiang and H. Z. Li, "Liquid drops hurdling barriers of various geometries," Adv. Mater. Interfaces **4**, 1700516 (2017).
[19]H. de Maleprade, A. Keiser, C. Clanet, and D. Quéré, "Friction properties of superhydrophobic ridges," J. Fluid Mech. **890**, A19 (2020).
[20]G. Dupeux, M. Le Merrer, C. Clanet, and D. Quéré, "Trapping Leidenfrost drops with crenelations," Phys. Rev. Lett. **107**, 114503 (2011).
[21]I. U. Vakarelski, N. A. Patankar, J. O. Marston, D. Y. C. Chan, and S. T. Thoroddsen, "Stabilization of Leidenfrost vapour layer by textured superhydrophobic surfaces," Nature **489**, 274–277 (2012).
[22]A. L. Biance, F. Chevy, C. Clanet, G. Lagubeau, and D. Quéré, "On the elasticity of an inertial liquid shock," J. Fluid Mech. **554**, 47–66 (2006).
[23]L. Mahadevan and Y. Pomeau, "Rolling droplets," Phys. Fluids **11**, 2449–2453 (1999).
[24]S. R. Hodges, O. E. Jensen, and J. M. Rallison, "Sliding, slipping and rolling: The sedimentation of a viscous drop down a gently inclined plane," J. Fluid Mech. **512**, 95–131 (2004).
[25]E. Yariv and O. Schnitzer, "Speed of rolling droplets," Phys. Rev. Fluids **4**, 093602 (2019).
[26]O. Schnitzer, A. M. J. Davis, and E. Yariv, "Rolling of nonwetting droplets down a gently inclined plane," J. Fluid Mech. **903**, A25 (2020).
[27]J. D. Smith, R. Dhiman, S. Anand, E. Reza-Garduno, R. E. Cohen, G. H. McKinley, and K. K. Varanasi, "Droplet mobility on lubricant-impregnated surfaces," Soft Matter **9**, 1772–1780 (2013).
[28]L. Quartier, B. Andreotti, S. Douady, and A. Daerr, "Dynamics of a grain on a sandpile model," Phys. Rev. E **62**, 8299–8307 (2000).